



Reactivity of a dichlorophosphido complex. Nucleophilic substitution reactions at metal coordinated phosphorus



Rakesh A. Rajagopalan, Arumugam Jayaraman, Brian T. Sterenberg*

Department of Chemistry and Biochemistry, University of Regina, 3737 Wascana Parkway, Regina, Saskatchewan S4S 0A2, Canada

ARTICLE INFO

Article history:

Received 30 January 2014

Received in revised form

18 February 2014

Accepted 26 February 2014

Keywords:

Phosphinidene

Alkoxyphosphinidene

Nucleophilic substitution

Metal-mediated synthesis

ABSTRACT

Reaction of the dichlorophosphido complex $[\text{Cp}^*\text{Mo}(\text{CO})_3(\text{PCl}_2)]$ (**1**) with AlCl_3 leads to the bimetallic bridging P_2Cl_3 complex $[(\text{Cp}^*\text{Mo}(\text{CO})_3)_2(\mu\text{-P}_2\text{Cl}_3)][\text{AlCl}_4]$ (**2**), which is formed via a Lewis-acid assisted nucleophilic substitution reaction, and not via a chlorophosphinidene intermediate. A similar reaction with external nucleophile PPh_3 leads to $[\text{Cp}^*\text{Mo}(\text{CO})_3(\text{P}(\text{Cl})\text{PPh}_3)][\text{AlCl}_4]$ (**3**), which can be viewed as a phosphine coordinated chlorophosphinidene complex. Addition of two equivalents each of PPh_3 and AlCl_3 leads a double chloride displacement, and formation of the known triphosphenium salt $[\text{Ph}_3\text{PPPh}_3][\text{AlCl}_4]$. In this reaction the dichlorophosphido complex effectively act as a source of P^+ . Reaction of **1** with alkoxides leads to alkoxyphosphido complexes $[\text{Cp}^*\text{Mo}(\text{CO})_3\{\text{P}(\text{OR})\text{Cl}\}]$ ($\text{R} = p\text{-}t\text{-butyl}$ phenoxy, menthoxy). These complexes serve as precursors to transient alkoxy phosphinidenes $[\text{Cp}^*\text{Mo}(\text{CO})_3\{\text{POR}\}]^+$, which can be trapped with alkynes. A computational study on the chloro, alkoxy, and related amino and alkyl phosphinidenes shows that chloro and alkoxy phosphinidenes have minimal π -donation to P from Cl or OR, in contrast to stable aminophosphinidenes, which have significant N to P π -donation.

© 2014 Elsevier B.V. All rights reserved.

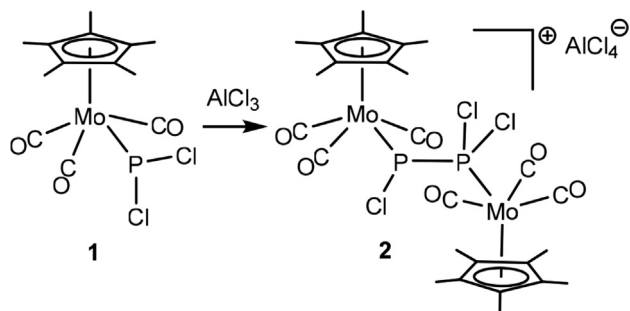
Introduction

Chloride abstraction is now a well established route to cationic terminal phosphinidene complexes, but phosphinidene complexes formed via this route are thus far limited to stable amino-phosphinidenes [1–3] and a transient alkyl phosphinidene [4]. In contrast, transient neutral terminal phosphinidene complexes have been described with a much wider variety of substituents on phosphorus, including alkyl and aryl [5], amino [6], alkoxy [7], chloro [8], and fluoro [9] substituents. Pikies has also made extensive studies of phosphanylphosphinidenes, however, these ligands most frequently bind in a side-on fashion, and are classified as nucleophilic [10]. The cationic electrophilic phosphinidene complexes show similar reactivity to transient neutral electrophilic phosphinidene [4,11], with some exceptions [12]. However, they have the advantages of shorter synthetic routes and can be generated at lower temperatures. We were interested in expanding the range of possible P substituents. Of particular interest to us is a

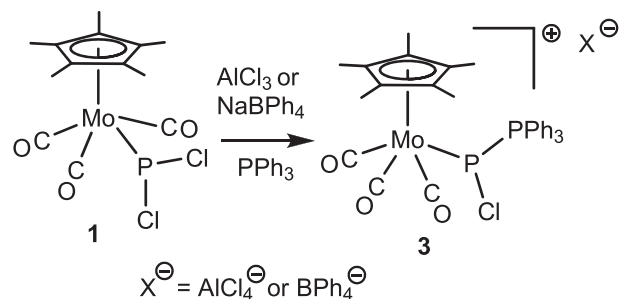
simple route to P–Cl phosphinidenes, because they can directly provide products, such as P-heterocycles and C–H activation products, containing a P–Cl bond ready for further substitution. This led us to explore the chemistry of dichlorophosphido complexes, which are potential precursors to cationic chloro–phosphinidene complexes. Terminal dichlorophosphido complexes are relatively rare [13–15], however the reactivity of the known complexes has been well explored, and typical reactions include oxidation of the lone pair, coordination to Lewis acids, and reductive coupling [16]. Iron PCl_2 complexes have also been used to form phospho-alkenes via nucleophilic substitution–dehydrohalogenation sequences [15]. As far as we know, direct halide abstraction as a route to chlorophosphinidene complexes has not been attempted, although a neutral transient chlorophosphinidene has been prepared by a different route [8]. Of known PCl_2 complexes, we were drawn to $[\text{Cp}^*\text{Mo}(\text{CO})_3(\text{PCl}_2)]$, reported by Malisch [13], because the synthesis is straightforward, and because it is analogous to the well studied phosphinidene precursor $[\text{Cp}^*\text{Mo}(\text{CO})_3\{\text{P}(\text{Cl})\text{N-}i\text{-Pr}_2\}]$. Here we describe the reaction chemistry of this complex with respect to chloride abstraction and substitution, and its utility as a precursor to phosphinidene complexes.

* Corresponding author. Tel.: +1 306 585 4106.

E-mail address: brian.sterenberg@uregina.ca (B.T. Sterenberg).



Scheme 1.



Scheme 3.

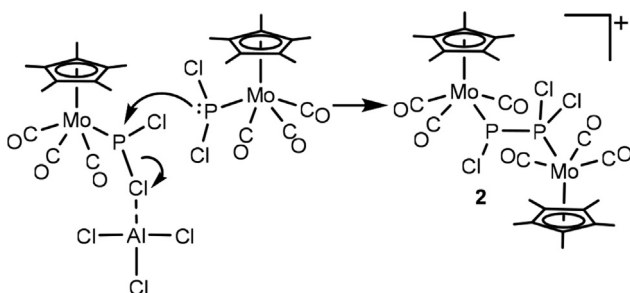
Results

Compound synthesis and characterization

The dichlorophosphido complex $[\text{Cp}^*\text{Mo}(\text{CO})_3(\text{PCl}_2)]$ (**1**) was synthesized from $\text{Cp}^*\text{Mo}(\text{CO})_3$ and PCl_3 using a modification of the published procedure [13]. The IR spectrum of **1** shows carbonyl stretching bands at 2018, 1951 and 1931 cm^{-1} and ^{31}P NMR spectrum shows a singlet at δ 408, matching reported values.

Abstraction of chloride from **1** was attempted using AlCl_3 , AgBF_4 and NaBPh_4 . All reagents led to the same metal complex **2** as the sole phosphorus containing product, with only the counterions differing. The ^{31}P NMR spectrum of **2** shows doublets at δ 318 and 258, each having a coupling constant of 528 Hz. The large P–P coupling constant indicates a direct P–P bond between two chemically inequivalent P atoms. The IR spectrum shows three carbonyl stretches at 2020, 1932 and 1953 cm^{-1} , in a pattern consistent with a $\text{Cp}^*\text{Mo}(\text{CO})_3\text{X}$ unit. The ^1H NMR spectrum shows peaks at δ 1.95 and 1.89 for two chemically different Cp^* groups. The ^{13}C NMR spectrum shows six carbonyls, and two Cp^* groups, confirming that there are two chemically non-equivalent $\text{Cp}^*\text{Mo}(\text{CO})_3$ units. The electrospray mass spectrum shows an isotope pattern ($m/z = 780\text{--}809$) that corresponds to the predicted masses for $\text{C}_{26}\text{H}_{30}\text{O}_6\text{P}_2\text{Cl}_3\text{Mo}_2^+$. Based on these data, the structure of **2** is assigned as a bimetallic complex containing a bridging P_2Cl_3 ligand and an overall +1 charge, which results from the displacement of chloride from one molecule of the dichlorophosphido ligand of **1** by a second equivalent of **1** (Scheme 1).

The observed product could indicate formation of a transient chlorophosphinidene, followed by its coordination by a second equivalent of **1**. In order to test this possibility, the chloride abstraction reaction was carried out in the presence of an alkyne trapping reagent. Reaction with alkynes to form phosphirenes is considered a characteristic reaction of terminal phosphinidene complexes [17]. However, in this attempted trapping reaction, compound **2** was the only observed product, and no phosphirene complex was detected, even with a large excess of alkyne and high



Scheme 2.

dilution. This suggests that **2** does not form via a phosphinidene intermediate, but by another mechanism. We suggest that **2** forms via a Lewis acid assisted nucleophilic substitution mechanism (Scheme 2).

In order to provide support for this mechanism, the reaction was carried out in the presence of an external nucleophile. Abstraction of chloride from **1** in the presence of one equivalent of triphenylphosphine leads to the triphenylphosphine coordinated chlorophosphinidene complex $[\text{Cp}^*\text{Mo}(\text{CO})_3\{\text{P}(\text{Cl})(\text{PPh}_3)\}][\text{X}]$ (**3**) (Scheme 3). Note that PPh_3 does not react with **1** in the absence of a chloride abstractor. The ^{31}P NMR spectrum of **3** shows two doublets at δ 179 and δ 37.9, both of which show a coupling constant of 454 Hz. The large coupling constant indicates a direct P–P bond. The IR spectrum of **3** shows three carbonyl stretches at 2019, 1972 and 1934 cm^{-1} , which indicate that the molybdenum center has retained three carbonyl ligands. Compound **3** has been structurally characterized, and an ORTEP diagram of the cation is shown in Fig. 1. The structure of the cation consists of a four legged piano stool, with three legs occupied by carbonyls and the fourth by the $\text{P}(\text{Cl})(\text{PPh}_3)$ unit. The metal bound P is trigonal pyramidal. The PPh_3 is coordinated to the metal bound P, and is directed away from the Cp^* ring, while the chloro group is directed such that the P–Cl bond is nearly parallel to the Cp^* ring. In this position, the Cl atom lies directly between the bulky Cp^* and PPh_3 groups. The reactivity of **1** towards nucleophiles, but not towards alkynes, supports the proposed Lewis acid assisted nucleophilic substitution mechanism.

Interestingly, the nucleophilic substitution reaction that leads to **3** can be repeated a second time, leading to the displacement of the second chloride with PPh_3 (Scheme 4). However, the formation of

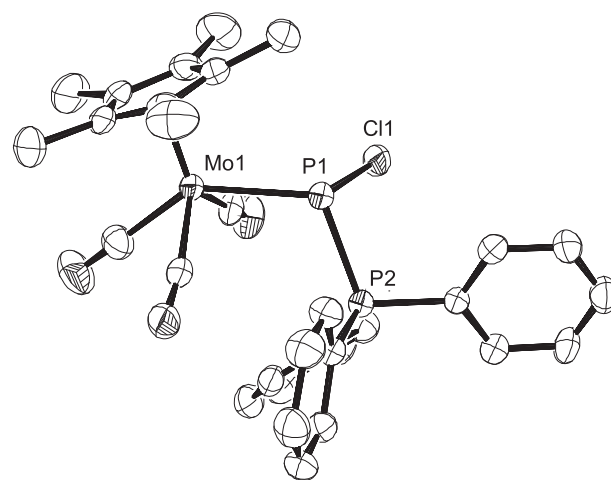
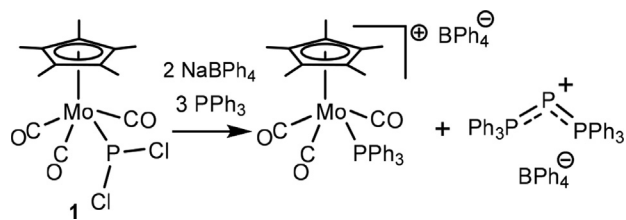


Fig. 1. ORTEP diagram showing one of two crystallographically non-equivalent cations of **3**. Hydrogen atoms and the counterion have been omitted for clarity. Selected distances and angles: Mo1–P1 = 2.531(1), P1–P2 = 2.196(1), P1–Cl(1) = 2.102(1), Mo1–P1–P2 = 112.51(5), Mo1–P1–Cl1 = 108.94(5), Cl(1)–P(1)–P(2) = 94.41(5).



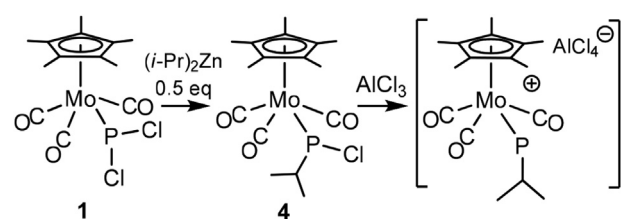
Scheme 4.

the second P–P bond is accompanied by dissociation from the metal complex. Thus, reaction of **1** with two equivalents of PPh₃ and two equivalents of NaBPh₄ leads to Ph₃PPPPh₃⁺, which was previously synthesized by Schmidpeter et al. from PCl₃, PPh₃, and AlCl₃ [18]. The fate of the metal fragment in this reaction is not known. However, if the same reaction is carried out with an additional equivalent of PPh₃, the Cp*Mo(CO)₃⁺ fragment can be trapped, forming the known complex [Cp*Mo(CO)₃PPh₃]⁺ [19].

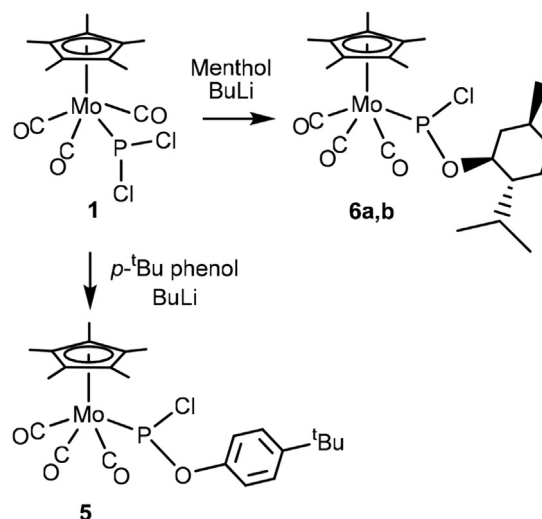
Although the dichlorophosphido complex **1** does not serve as a precursor to the chlorophosphinidene, its facile nucleophilic substitution reactions led us to consider its use as a precursor to other phosphido complexes. For example, reaction of **1** with an alkyl nucleophile can be used as a synthetic route to chloro alkyl phosphido complexes, which in turn serve as precursors to alkyl phosphinidenes [4]. We have applied this methodology to the known chlorophosphido complex [Cp*Mo(CO)₃(P(Cl)(*i*-Pr))] (**4**), previously formed from *i*-PrPCl₂ and [Cp*Mo(CO)₃]⁻. Reaction of **1** with isopropyl magnesium chloride led to a mixture of unreacted starting material, mono- and di-substitution. Diisopropylzinc, however, is more selective, and leads to **4** as the major product (Scheme 5). Abstraction of chloride from **4** leads to the transient alkyl phosphinidene complex [Cp*Mo(CO)₃{P(*i*-Pr)}][AlCl₄]. Some of the reaction chemistry of this alkyl phosphinidene, formed via a different route, was described previously [4].

Compound **1** is also an effective precursor to phenoxy- and alkoxy-phosphido complexes. Reaction of **1** with para-*t*-butyl phenoxide leads to the phenoxy phosphido complex [Cp*Mo(CO)₃(P(Cl)(*p*-OC₆H₄C(CH₃)₃))] (**5**) (Scheme 6). Similarly, reaction of **1** with (–)-mentoxide anion leads to the alkoxy phosphido complex [Cp*Mo(CO)₃(P(Cl)(OC₁₀H₁₉))] (**6a,b**). As a result of the chirality of the menthoxy group, **6** exists as two diastereomers as indicated by ³¹P NMR spectrum, which shows signals at δ 421 and δ 406 in a ratio of 27:73. Other alkoxy and phenoxy phosphido complexes, including those with the parent phenoxy and naphthoxy groups have also been synthesized, but they formed oils that were difficult to purify. As a result, we focused on **5** and **6**, which are crystalline.

The chloride group on the phosphido complexes **5** and **6** can be readily abstracted using AlCl₃, however attempts to observe stable alkoxy phosphinidene complexes were not successful. At low temperatures, the abstraction reaction is suppressed, but at higher temperatures, decomposition is rapid. In the absence of trapping reagents, decomposition of alkoxy or aryloxy phosphinidenes led to [Cp*Mo(CO)₃{PH(OR)₂}]⁺ (identified by electrospray MS), along



Scheme 5.



Scheme 6.

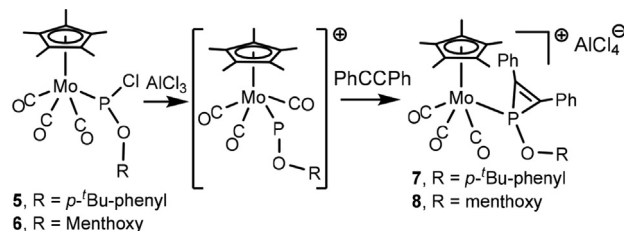
with other products that could not be identified or isolated. The observed product presumably results from nucleophilic attack on the phosphinidene complex by the O atom of a second equivalent of the phosphinidene, followed by hydrolysis by adventitious water. The fate of the second metal complex in this reaction is not known.

Although stable phenoxy and alkoxy phosphinidenes could not be observed, transient phosphinidenes are readily identified through trapping reactions. Abstraction of chloride from compounds **5** or **6** with AlCl₃ in the presence of diphenylacetylene leads to the expected phosphirene complexes [Cp*Mo(CO)₃(P(OC₆H₄C(CH₃)₃)C(Ph)C(Ph))][AlCl₄] (**7**) and [Cp*Mo(CO)₃(P(OC₁₀H₁₉)C(Ph)C(Ph))][AlCl₄] (**8**) (Scheme 7). The ³¹P NMR spectra of **7** and **8** show singlets at δ –21.1 and –32.6 respectively, in the high field region expected for phosphirene complexes. Because the P centre in **8** is no longer stereogenic, a single isomer of **8** is formed from two diastereomers of **6**. These resonances are deshielded compared to other comparable phosphirene complexes [2,20] as a result of the alkoxy or aryloxy substituent. Since reaction with alkynes to form phosphirenes is considered a characteristic reaction of terminal electrophilic phosphinidene complexes [17], the observed products are strong supporting evidence for transient cationic alkoxy-phosphinidenes. These are the first known cationic alkoxy and aryloxy phosphinidene complexes.

Attempts to trap the alkoxy and aryloxy phosphinidenes with ferrocene were not successful, and the products were the same as those obtained in absence of a trapping reagent. This contrasts with the alkyl phosphinidene [Cp*Mo(CO)₃{P(*i*-Pr)}]⁺, which inserts into a C–H bond of ferrocene [4].

Computational study

In order to gain further insight into the relative stabilities of the various cationic phosphinidene compounds, a computational study



Scheme 7.

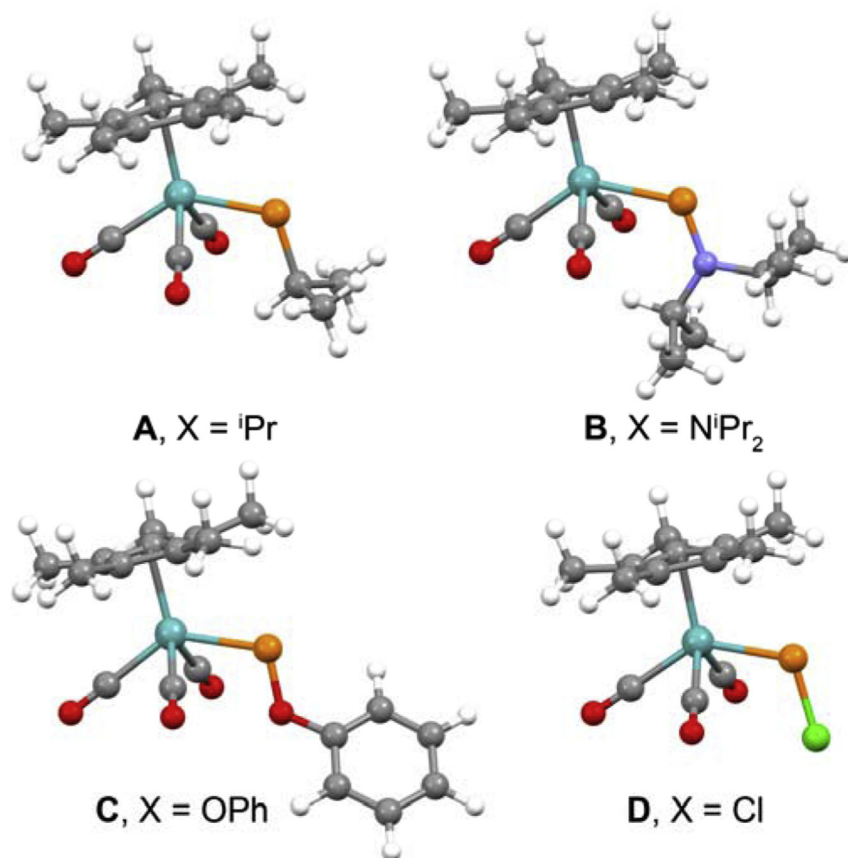


Fig. 2. Optimized structures of **A–D**. Selected bond distances (Å) and angles: **A**, Mo–P = 2.397, P–C = 1.873, Mo–P–C = 115.76. **B**, Mo–P = 2.476, P–N = 1.671, Mo–P–N = 119.65. **C**, Mo–P = 2.423, P–O = 1.658, Mo–P–O = 108.98. **D**, Mo–P = 2.384, P–Cl = 2.065, Mo–P–Cl = 114.02.

has been carried out on a series of cationic complexes with various P substituents. Neutral terminal phosphinidene complexes have been extensively studied computationally, including studies on electrophilic versus nucleophilic natures of phosphinidenes [21], specific studies on transient electrophilic phosphinidenes [22,23], stable nucleophilic phosphinidenes [24], and stable electrophilic phosphinidenes [25]. Cationic complexes, including $[\text{Cp}^*\text{Mo}(\text{CO})_3(\text{PCH}_3)]^+$, have been examined by Pandey et al. using DFT [26]. However, the role of the P substituent in the stability of cationic phosphinidenes has not been directly addressed.

DFT calculations were carried out on the complexes $[\text{Cp}^*\text{Mo}(\text{CO})_3(\text{PX})]^+$, where X = i -Pr (**A**), N^i -Pr₂ (**B**), OPh (**C**), and Cl (**D**), at the B3LYP level of theory [27]. Mayer bond orders [28] and NBO charges [29] were calculated, and fragment molecular orbital (FMO) analysis [30,31] was carried out for each of the complexes. Optimized structures are shown in Fig. 2. The optimized structure of aminophosphinidene complex **B** provided a good agreement with the experimentally determined structure [1] (see Table S1 of Supporting Information).

These cationic electrophilic phosphinidene complexes can be viewed as neutral singlet phosphinidenes (PX) coordinated via a dative bond to a cationic metal complex, or as metallaphosphenium ions. Either formulation places a formal positive charge and an empty p_z orbital at P. The electron deficiency at P is alleviated by π donation from a heteroatom substituent or by metal-to-P π -back donation (Fig. 3). Computed Mayer bond orders (Table 1) give a measure of X to P π donation, while the M–P bond order gives a measure of M-to-P π -back donation. The P- i -Pr complex has no substituent non-bonding pairs, and as expected, has the lowest P–X bond order. The PNR₂ complex has the highest P–X bond

order, reflecting the strong N–P π overlap. The PCl and POPh complexes are intermediate between these extremes, showing evidence for weak X–P overlap. The Mo–P bond orders show that the P- i -Pr and P–Cl phosphinidenes are the strongest π -acceptors, while PN- i -Pr₂ and POPh are weaker π -acceptors. A similar trend was observed in calculations on $\text{Cr}(\text{CO})_5\text{PR}$ (R = H, CH₃, SiH₃, NH₂, PH₂, OH, and SH), where PH, PCH₃, and PSiH₃ were shown to be significant π -acceptor ligands, while POH, PNH₂, and PSH were much weaker π acceptors [23].

Computed NBO charges for **A–D** are shown in Table 2. The charges listed are the summed charges on the $[\text{Cp}^*\text{Mo}(\text{CO})_3]$ fragment, the charge on P, and summed charges on phosphorus substituent. The NBO charges show a significant positive charge localized at P in all of the complexes, consistent with the bonding model. The summed charge on the P substituent gives an indication of the electron withdrawing/electron donating abilities of the substituent. It is assumed based on our bonding model that electron withdrawing is inductive via the sigma bond, and depends on

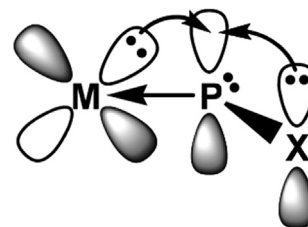


Fig. 3. Heteroatom to P π donation and M-to-P π -back donation in phosphinidene complexes.

Table 1
Computed Mayer bond orders for compounds **A–D**.

Compound	Substituent	Mo–P	P–X
A	<i>i</i> -Pr	1.326	0.908
B	<i>N-i</i> -Pr ₂	1.016	1.381
C	OPh	1.163	1.084
D	Cl	1.302	1.070

relative electronegativities, while electron donation occurs via π overlap. Based on induction alone, the expected order of increasing negative charge on X would be $R < NR_2 < Cl < OR$. The calculated order is $NR_2 \ll Cl < R < OR$, clearly showing that NR_2 is a significant π donor to P, while the other substituents have much less π overlap. It is also noteworthy that the summed charge on the alkyl group is greater than that on chloro, contrary to expectation based on electronegativity, and suggesting that there is at least some Cl to P π donation.

The summed charge on the metal fragment gives an indication of the relative donor/acceptor abilities of the different phosphinidene ligands. The calculated ordering from strongest donor to strongest acceptor is $PNR_2 > POR > PR > PCl$. The positioning of PNR_2 as strongest donor/weakest acceptor suggests that strong N to P π donation precludes significant M to P π -back donation, resulting in a ligand that is primarily a σ donor, consistent with the bond order results. The PR and PCl complexes have significantly higher positive charge on the metal fragment, indicating that they act as π -acceptors. Because the alkyl substituent on PR has no non-bonding pair, there is no π overlap with the substituent, and the phosphorus p_z orbital is fully available to accept π -back donation from the metal. Based on the metal charge, PCl is an even stronger π acceptor than PR. On the other hand, POPh is only a weak π acceptor ligand, inducing a smaller positive charge on the metal than P-*i*-Pr or P-Cl. Weak π -back donation and weak O-to-P π donation means that the P atom in the POPh complex carries the highest positive charge. In the PCl and P-*i*-Pr complexes, the positive charge is delocalized onto the metal by π -back donation, while in the PN-*i*-Pr₂ complex, it is delocalized onto N by π donation. As a result, the POPh phosphinidene is expected to be most electrophilic at P.

Fragment molecular orbital (FMO) analysis allows us to further decompose the M–P interaction into σ -donation and π -back donation components. In all of these complexes, the M–P σ -interaction occurs from the highest occupied fragment orbital (HOFO) of the phosphinidene fragment to the lowest unoccupied fragment orbital (LUFO) of the $[Cp^*Mo(CO)_3]^+$ fragment (Fig. 4[i]). The changes in occupancies to the fragment orbitals upon complex formation allow us to gauge relative bond strength. The HOFO of the phosphinidene fragment, used to form the σ bond, (Fig. 4) shows a similar drop in occupancy across the four complexes, indicating that the σ -bond strength is approximately equal across the four complexes. Similarly, the increase in occupancy for the LUFO of the metal fragment is nearly the same across all four complexes.

The π interaction occurs from the HOFO-1 of $[Cp^*Mo(CO)_3]^+$ to the LUFO (the empty p_z orbital of P) on the phosphinidene fragment (Fig. 4[ii]). The increase in the LUFO occupancy, and the decrease in

Table 2
Computed NBO charges of compounds **A–D**.

Compound	Substituent	Charge		
		$[Cp^*Mo(CO)_3]$	P	X
A	<i>i</i> -Pr	0.260	0.933	–0.192
B	<i>N-i</i> -Pr ₂	0.113	0.968	–0.082
C	OPh	0.197	1.124	–0.321
D	Cl	0.339	0.823	–0.161

the HOFO-1 occupancy show that the π interaction is weaker than the σ interaction, as expected, but also that the π interaction varies significantly across the four complexes, being weakest for $X = NR_2$, and strongest for $X = i$ -Pr and Cl. This further reinforces the conclusions drawn from bond orders and NBO charges that M to P π -back donation is strongest in the chloro and alkyl phosphinidenes, and weakest in the aminophosphinidene. The phenoxy is intermediate.

Finally, the computed reaction energies (kcal/mol) to abstract chloride using $AlCl_3$ from their precursors to form complexes **A–D** show that all reactions are exothermic. Formation of the aminophosphinidene is by far the most exothermic at –33.1 kcal/mol. It is followed in order by POPh (–15.4 kcal/mol), P-*i*-Pr (–12.3 kcal/mol) and PCl (–7.1 kcal/mol).

Discussion

We have now examined cationic phosphinidene complexes with four different functional groups on P, formed via chloride abstraction. Of these four, aminophosphinidenes are stable [1], alkyl [4] and alkoxy phosphinidenes are transient and can be trapped, while chlorophosphinidenes could not be formed by this route. Our inability to observe stable alkoxy or aryloxy phosphinidenes suggests that the alkoxy and aryloxy groups do not provide sufficient π -overlap to stabilize the electron deficient phosphorus, making them comparable to the alkyl phosphinidene. However, in contrast to the analogous alkyl phosphinidene, the alkoxy phosphinidenes do not activate the C–H bonds of ferrocene [4], suggesting that they may be less electrophilic than the alkyl phosphinidene. Our inability to obtain evidence for even a transient chlorophosphinidene suggested that Cl–P π overlap is weak or non-existent, and that the chloro substituent may further destabilize the phosphinidene.

The computational study clearly shows why the aminophosphinidene is the only stable and isolable complex. Its formation is far more exothermic than the formation of any of the other phosphinidenes. The key difference is the extent of N to P π -donation, which is far greater than the π donation in any of the other complexes, and we attribute its stability to this π -stabilization. Previous computational studies have shown that in π -donor substituted free phosphinidenes, the ground spin state depends on the extent of π -overlap of the non-bonding electrons of π -donor substituent with an empty p orbital of phosphorus [32]. In amino phosphinidenes, effective π -overlap favours the singlet state, but in alkoxy and halo phosphinidenes, less effective π -overlap favours the triplet ground state. The cationic metal complexes described here show the same trend: strong π donation for the aminophosphinidene, and weak π -donation in phenoxy and chloro phosphinidenes. The same trend is observed experimentally in related phosphonium ions, which are generally stable only when at least one substituent is an amino group [33]. Clearly, the amino group is uniquely effective at stabilizing electron deficient phosphorus centers.

The extent of M to P π -back donation also varies considerably between the different complexes. In the case of the aminophosphinidene, strong N–P π donation appears to preclude strong M to P π -back donation. In contrast, the chloro and alkyl phosphinidenes, which have weak or no X–P π overlap, are stronger π acceptors from the metal. Although π -back donation effectively alleviates positive charge on P in the alkyl and chloro phosphinidenes (Table 2), it does not appear to have the same stabilizing effect as N–P overlap.

Interestingly, the phenoxy phosphinidene has neither strong O–P overlap nor metal back donation. This suggests that repulsion by the oxygen lone pairs make π -back donation less favourable even if O–P π overlap is weak. The lack of π donation results in the highest positive charge at P, suggesting that the phenoxy phosphinidene

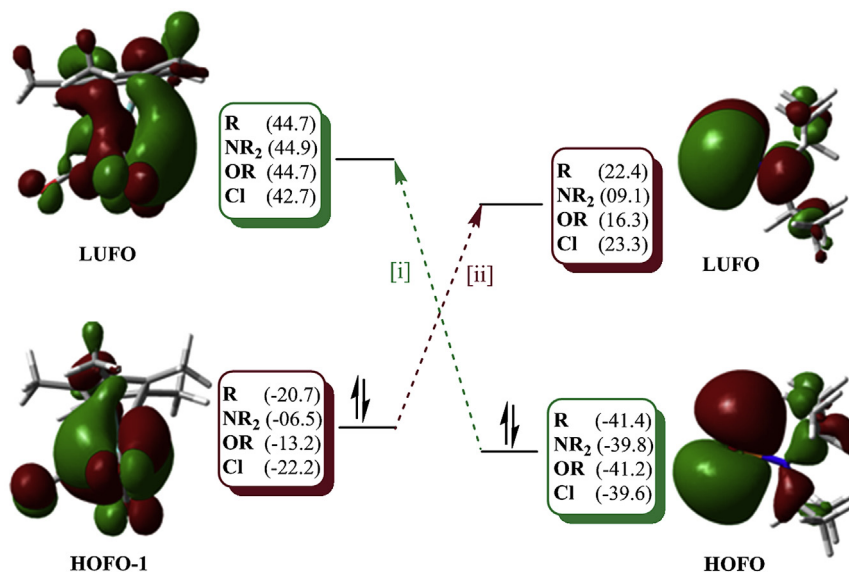


Fig. 4. Isosurface plots (isovalue: 0.02) of selected fragment molecular orbitals (FOs) of $[\text{Cp}^*\text{Mo}(\text{CO})_3]^+$ and $\text{P}(\text{N-}i\text{-Pr}_2)$ involved in σ -donation [i] and π back-donation [ii]. Isosurface plots of FOs of other complexes ($X = i\text{-Pr, OPh, Cl}$) are similar to those of the $\text{N-}i\text{-Pr}_2$ complex shown. The values in brackets correspond to the percent changes in FO occupancies upon formation of complexes **A–D** from their corresponding $[\text{Cp}^*\text{Mo}(\text{CO})_3]^+$ and PR fragments.

should be the most electrophilic. Its failure to activate the C–H bonds of ferrocene is therefore most likely not a result of insufficient electrophilicity, but rather a result of an alternative, more facile reaction, namely nucleophilic attack by the oxygen of a second equivalent of the phosphinidene complex.

Although the chlorophosphinidene is clearly the least stable complex in the series, its formation is still exothermic, and the calculations reveal no inherent reason for instability. In fact, its P atom carries less positive charge than the alkyl or phenoxy phosphinidenes. This suggests that it should have similar stability and reactivity to the alkyl or alkoxy phosphinidenes, and should thus be trappable. Our inability to generate it as a transient species and trap it is therefore likely not a result of inherent instability, but rather a result of alternate lower energy pathways that lead to substitution reactions, rather than abstraction. This alternate reaction, unique to the chlorophosphinidene, likely results from the lack of steric protection provided by the chloro substituent.

In conclusion, the dichlorophosphido complex does not serve as a precursor to a chlorophosphinidene, but undergoes Lewis acid assisted nucleophilic substitutions with weak nucleophiles, including itself and PPh_3 . Reactions with stronger nucleophiles serve as routes to substituted chlorophosphido complexes, precursors to phosphinidenes. We have used this route to generate alkyl, aryloxy and alkoxy phosphinidenes. Unlike amino phosphinidenes, alkoxy or aryloxy phosphinidenes are not stable, but can be readily trapped with alkynes and phosphines.

Experimental section

General comments

All procedures were carried out under a nitrogen atmosphere using standard Schlenk techniques or in an inert atmosphere glovebox. THF was distilled from Na/benzophenone. Dichloromethane and hexane were purified using solvent purification columns containing alumina (dichloromethane) or alumina and copper oxide catalyst (hexane). Deuterated chloroform was distilled from P_2O_5 . The NMR spectra were recorded in CDCl_3 using a Varian Mercury 300 spectrometer operating at 300.179 MHz (^1H), 75.479 MHz (^{13}C { ^1H }), and 121.515 MHz (^{31}P { ^1H }). Infrared spectra were recorded in

solution in THF or CH_2Cl_2 . Mass spectra were recorded using a Finnigan-Matt TSQ-700 mass spectrometer equipped with electrospray ionization and a Harvard syringe pump. Elemental analyses were carried out by the Analytical and Instrumentation Laboratory, Department of Chemistry, University of Alberta. Compounds **7** and **8** formed oils that could not be crystallized. As a result, satisfactory elemental analyses could not be obtained. Their formulations are supported by ESI mass spectrometry and NMR spectroscopy (see [Supporting Information](#) for spectra).

Compound synthesis

Synthesis of $[\text{Cp}^*\text{Mo}(\text{CO})_3(\text{PCl}_2)]$ (**1**)

Compound **1** was synthesized using a modification of the published procedure [13]. To pentamethylcyclopentadiene (0.52 g, 3.8 mmol, 0.60 mL) in 50 mL THF was added *n*-butyllithium (2.4 mL of 1.6 M solution in hexane, 3.8 mmol). Molybdenum hexacarbonyl (1.00 g, 3.78 mmol) was then added, and the resulting solution was heated under reflux for 16 h, resulting in an orange solution of $[\text{Cp}^*\text{Mo}(\text{CO})_3]$. This solution was added in small portions to a solution of phosphorus trichloride (1.03 g, 7.5 mmol, 0.66 mL) in 75 mL of THF at 0 °C. The reaction mixture was stirred for 30 min and the solvent was removed under reduced pressure at 0 °C. The orange residue obtained was extracted into 3 × 40 mL of pentane and the resulting solution was filtered. The pentane filtrate was concentrated to 10 mL and cooled to –30 °C, resulting in the formation of large orange crystals. The crystals obtained were collected and stored at –35 °C. Yield = 1.15 g, 73%. IR (THF solution, $\nu(\text{CO})$, cm^{-1}): 2018 s, 1952 s, 1932 s $^{31}\text{P}\{^1\text{H}\}$ NMR: δ 408.5. ^1H NMR: δ 1.96 (d, $J_{\text{HP}} = 9.0$ Hz, 15H, $\text{C}_5(\text{CH}_3)_5$).

Synthesis of $[\{\text{Cp}^*\text{Mo}(\text{CO})_3\}_2(\mu\text{-PCl}_3)][\text{AlCl}_4]$ (**2**)

The compound $[\text{Cp}^*\text{Mo}(\text{CO})_3(\text{PCl}_2)]$ (**1**; 20 mg, 0.047 mmol) was dissolved in CH_2Cl_2 (5.0 mL). The resulting solution was added to AlCl_3 (3 mg, 0.024 mmol) and stirred for 30 min. A slow colour change from orange to dark red was observed. The solvent was removed under reduced pressure and the residue obtained was extracted into CH_2Cl_2 (0.5 mL) and crystallized as orange crystals by slow diffusion of diethyl ether into the CH_2Cl_2 solution. Yield:

19.4 mg, 52.2%. IR (CH₂Cl₂ solution, $\nu(\text{CO})$, cm⁻¹): 2020 s, 1953 s, 1933 s. ³¹P{¹H} NMR: δ 318 (d, ¹J_{PP} = 527 Hz, MoPP), 258 (d, ¹J_{PP} = 528 Hz, MoPP). ¹H NMR: δ 5.29 (s, CH₂Cl₂), δ 2.16 (d, ¹J_{HP} = 1.5 Hz, 15H, C₅(CH₃)₅), 2.05 (s, 15H, C₅(CH₃)₅). ¹³C NMR: δ 233.2 (d, ¹J_{CP} = 8 Hz, MoCO), 227.7 (s, MoCO), 227.3 (d, ¹J_{CP} = 4 Hz, MoCO), 224.8 (s, MoCO), 224.4 (s, MoCO), 221.6 (s, MoCO), 110.9 (s, C₅(CH₃)₅), 108.4 (s, C₅(CH₃)₅), 11.1 (s, C₅(CH₃)₅), 10.7 (d, ¹J_{CP} = 4 Hz, C₅(CH₃)₅). MS (electrospray, CH₂Cl₂ solution): m/z = 789–809 (M⁺) (Fig. 5). Anal. Calcd for C₂₆H₃₀AlCl₇Mo₂P₂O₆·CH₂Cl₂: C, 30.81; H, 3.06. Found: C, 30.82; H, 3.16. Co-crystallized CH₂Cl₂ was observed in the ¹H NMR spectrum of the crystals.

Synthesis of [Cp*Mo(CO)₃{P(Cl)(PPh₃)}][AlCl₄] (3)

Compound **1** (20 mg, 0.047 mmol) and PPh₃ (12.5 mg, 0.047 mmol) were dissolved in CH₂Cl₂ (0.5 mL). The resulting solution was added to AlCl₃ (6 mg, 0.047 mmol) and stirred for 30 min. An immediate colour change from yellow to dark red was observed. The solvent was then removed under reduced pressure. The residue was extracted into CH₂Cl₂ (0.5 mL) and crystallized as yellow crystals by slow diffusion of diethyl ether into the CH₂Cl₂ solution. Yield: 24.6 mg, 63%. IR (THF solution, $\nu(\text{CO})$, cm⁻¹): 2017 s, 1967 s, 1932 s. ³¹P{¹H} NMR: δ 177 (d, ¹J_{PP} = 453 Hz, MoPP), 35.7 (d, ¹J_{PP} = 451 Hz, MoPP). ¹H NMR: δ 7.71–6.78 (multiplets, Ph), 1.88 (s, 15H, C₅(CH₃)₅). ¹³C NMR: δ 233.6 (dd, ¹J_{CP} = 10 Hz, ²J_{CP} = 3 Hz, MoCO), 228.1 (s, MoCO), 221.5 (s, MoCO), 134.7 (d, ¹J_{CP} = 4 Hz, Ph), 133.9 (s, Ph), 133.8 (s, Ph), 133.5 (dd, ¹J_{CP} = 15 Hz, ²J_{CP} = 4 Hz, Ph), 130.5 (d, ¹J_{CP} = 12 Hz, Ph), 120.6 (dd, ¹J_{CP} = 58 Hz, ²J_{CP} = 6 Hz, ipso-Ph), 108.5 (s, C₅(CH₃)₅), 10.7 (d, ¹J_{CP} = 6 Hz, C₅(CH₃)₅). MS (electrospray, CH₂Cl₂ solution): m/z = 639–652 (M⁺). Anal. Calcd. for C₃₁H₃₀MoO₃Cl₅AlP₂: C, 45.80; H, 3.72. Found: C, 45.70; H, 3.69.

Synthesis of [Cp*Mo(CO)₃{P(Cl)(i-Pr)}] (4)

A solution of Zn(*i*-Pr)₂ was prepared by dropwise addition of *i*-PrMgCl (0.734 mL of 2 M solution in THF, 1.460 mmol) to a solution of ZnCl₂ (100 mg, 0.734 mmol) in 5 mL of THF, followed by 30 min of stirring. Compound **1** (100 mg, 0.239 mmol) was dissolved in THF (25 mL). A portion of the Zn(*i*-Pr)₂ solution (0.922 mL of 0.13 M solution in THF, 0.119 mmol) was added dropwise to the solution of **1**, resulting in an immediate colour change from orange to dark red. After the addition was completed, the resulting solution was stirred for 30 min and the solvent was removed under reduced pressure. The dark red residue was extracted in pentane (20 mL) and filtered. The pentane was removed under reduced pressure and the resulting orange oil was dissolved in minimum amount of hexane. The hexane solution was then kept at -35 °C for two days, resulting in the formation of orange crystals. Yield: 50.9 mg, 50%. IR (hexane solution, $\nu(\text{CO})$, cm⁻¹): 2007 s, 1944 s, 1915 s. ³¹P{¹H} NMR: δ 269.7. ¹H NMR: δ 2.31 (d sept, 1H, ²J_{HP} = 27.9 Hz, ³J_{HH} = 7.0 Hz, CH(CH₃)₂), 1.96 (s, 15H, C₅(CH₃)₅), 1.37 (dd, 3H, ³J_{HP} = 23.4 Hz, ³J_{HH} = 7.2 Hz, CH(CH₃)₂), 1.36 (d, 3H, ³J_{HH} = 6.9 Hz, CH(CH₃)₂). ¹³C NMR: δ 236.8 (d, ²J_{CP} = 9 Hz, MoCO), 229.1 (s, MoCO), 225.0 (s, MoCO), 106.6 (s, C₅(CH₃)₅), 36.4 (d, ¹J_{CP} = 47 Hz, PCH(CH₃)₂), 22.7 (d, ²J_{CP} = 18 Hz,

PCH(CH₃)₂), 21.3 (d, ²J_{CP} = 3 Hz, PCH(CH₃)₂), 10.6 (d, ¹J_{CP} = 6 Hz, C₅(CH₃)₅). Anal. Calcd for C₁₆H₂₂O₃PClMo: C, 45.25; H, 5.22. Found: C, 45.06; H, 5.34.

Synthesis of [Cp*Mo(CO)₃{P(Cl)(OC₆H₄C(CH₃)₃)} (5)

Butyl lithium (0.749 mL of 1.6 M solution in THF, 1.198 mmol) was added dropwise to a solution of 4-*tert*-butylphenol (180 mg, 1.198 mmol) in THF (5 mL). The solution was stirred for 30 min. Compound **1** (500 mg, 1.198 mmol) was dissolved in THF (25 mL). The 4-*tert*-butylphenoxide ion solution was then added dropwise, resulting in gradual colour change from orange to dark red. The solvent was removed under reduced pressure and the dark residue obtained was extracted in pentane (10 mL) and filtered. The pentane was removed under reduced pressure and the residue was dissolved in minimum amount of hexane. The hexane solution was then cooled to -35 °C for 24 h, resulting in the formation of large dark red crystals. Yield: 558 mg, 87.7%. IR (hexane solution, $\nu(\text{CO})$, cm⁻¹): 2017 s, 1953 s, 1931 s. ³¹P{¹H} NMR: δ 403.3. ¹H NMR: δ 7.32 (dm, 2H, ³J_{HH} = 9 Hz, Ph), 7.10 (ddm, 2H, ³J_{HH} = 9 Hz, ⁴J_{HP} = 3 Hz, Ph), 1.98 (d, 15H, ¹J_{HP} = 0.6 Hz, C₅(CH₃)₅), 1.29 (s, 9H, C(CH₃)₃). ¹³C NMR: δ 245.0 (s, MoCO), 233.4 (d, ²J_{CP} = 7 Hz, MoCO), 226.1 (s, MoCO), 155.6 (d, ²J_{CP} = 3 Hz, ipso-Ph), 145.2 (d, ¹J_{CP} = 1 Hz, ipso-Ph), 125.2 (s, Ph), 117.5 (d, ³J_{PC} = 9 Hz, Ph), 104.9 (s, C₅(CH₃)₅), 30.4 (s, C(CH₃)₃), 9.28 (d, ¹J_{CP} = 7 Hz, C₅(CH₃)₅). Anal. Calcd for C₂₃H₂₈O₄ClMoP: C, 52.04; H, 5.32. Found: C, 51.92; H, 5.80.

Synthesis of [Cp*Mo(CO)₃{P(Cl)(OC₁₀H₁₉)} (6)

Butyl lithium (74.9 μ L of 1.6 M solution in THF, 0.119 mmol) was added dropwise to a solution of (-)-menthol (18.7 mg, 0.119 mmol) in THF (5 mL). The solution was stirred for 30 min. Compound **1** (50 mg, 0.119 mmol) was dissolved in THF (10 mL). The menthoxide solution then added dropwise, resulting in an immediate colour change from orange to dark red. The reaction solution was stirred for 30 min and the solvent was removed under reduced pressure. The dark red residue was extracted into pentane (10 mL) and filtered. The pentane was removed and the dark oily residue was redissolved in minimum amount of hexane. The hexane solution was then cooled to -35 °C, resulting in the formation of dark red crystals. Yield: 40.2 mg, 62.5%. IR (CH₂Cl₂ solution, $\nu(\text{CO})$, cm⁻¹): 2009 s, 1939 s, 1919s. ³¹P{¹H} NMR: δ 421.4 (27%), 406.3 (73%). ¹H NMR (major diastereomer): 3.68 (ddt, 1H, ³J_{HP} = 32.7 Hz, ³J_{HH} = 11.1 Hz, ³J_{HH} = 4.5 Hz, H_A menthol), 2.37–2.07 (broad multiplets, menthol), 1.89 (s, 15H, C₅(CH₃)₅), 1.77–1.24 (broad multiplets, menthol), 0.91 (d, 3H, ³J_{HH} = 6.6 Hz, CH(CH₃)₂(menthol)), 0.87 (d, 3H, ³J_{HH} = 7.2 Hz, CH₃ (menthol)), 0.77 (d, ³J_{HH} = 6.9 Hz, CH(CH₃)₂ (menthol)). ¹³C NMR (major diastereomer): δ 246.3 (s, MoCO), 235.2 (d, ²J_{CP} = 7 Hz, MoCO), 227.3 (s, MoCO), 106.0 (s, C₅(CH₃)₅), 82.3 (d, ²J_{CP} = 5 Hz, menthol C₁), 49.4 (s, menthol C₂), 42.5 (s, menthol C₆), 34.4 (s, menthol C₄), 31.9 (s, menthol C₅), 24.8 (s, (CH₃)₂C, menthol), 23.1 (s, menthol C₃), 22.3 (s, menthol CH₃), 21.3 (s, menthol CH(CH₃)₂), 16.0 (s, menthol CH(CH₃)₂), 10.5 (d, ¹J_{PC} = 6 Hz, C₅(CH₃)₅). Anal. Calcd for C₂₃H₃₄O₄PClMo: C, 51.45; H, 6.38. Found: C, 51.06; H, 6.40.

Synthesis of [Cp*Mo(CO)₃{P(OC₆H₄C(CH₃)₃)C(Ph)C(Ph)}][AlCl₄] (7)

[Cp*Mo(CO)₃{P(Cl)(OC₆H₄C(CH₃)₃)} (5; 50 mg, 0.0941 mmol) and diphenylacetylene (16.7 mg, 0.0941 mmol) were dissolved in CH₂Cl₂ (5.0 mL). The resulting solution was added to AlCl₃ (12.5 mg, 0.0941 mmol) and stirred for 30 min. The solvent volume was reduced to ~2 mL, and pentane (10 mL) was added to the concentrated reaction solution with rapid stirring, resulting in the formation of a dark oil. The supernatant was decanted and the oil was washed with pentane (5.0 mL) and dried under vacuum. Yield: 24 mg, 38.4%. IR (CH₂Cl₂ solution, $\nu(\text{CO})$, cm⁻¹): 2017 s, 1979 s, 1951 s. ³¹P{¹H} NMR: -21.4, ¹H NMR: 7.6–6.8 (multiplets, Ph), 7.12

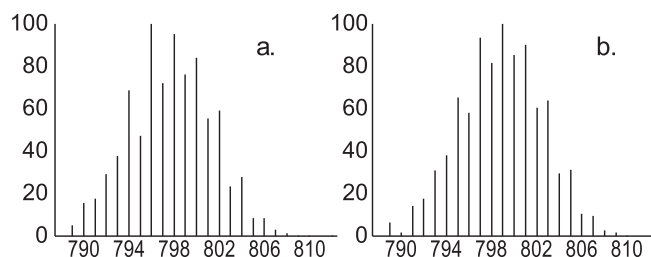


Fig. 5. Electro spray MS of **2** showing molecular ion cluster. a. Calculated for C₂₆H₃₀Cl₃Mo₂O₆P₂. b. Experimental.

(dm, 2H, $^3J_{\text{HH}} = 9$ Hz, Ph), 6.66 (ddm, 2H, $^3J_{\text{HH}} = 9$ Hz, $^4J_{\text{HP}} = 3$ Hz, Ph), 2.12 (s, $\text{C}_5(\text{CH}_3)_5$), 1.08 (s, 9H, $\text{C}(\text{CH}_3)_3$). ^{13}C NMR: δ 226.3 (s, MoCO), 225.7 (d, $J_{\text{CP}} = 40$ Hz, MoCO), 149.6 (d, $J_{\text{CP}} = 2$ Hz, *ipso*-Ph), 148.4 (d, $J_{\text{CP}} = 17$, phosphirene ring C), 146.3 (d, $J_{\text{CP}} = 16$, Ph), 132.7 (s, Ph), 130.1 (s, Ph), 129.3 (d, $J_{\text{CP}} = 6$ Hz, Ph), 127.3 (d, $J_{\text{CP}} = 2$ Hz, Ph), 126.6 (s, Ph), 120.8 (d, $J_{\text{CP}} = 5$ Hz, *ipso*-Ph), 110.1 (s, $\text{C}_5(\text{CH}_3)_5$), 31.4 (s, $\text{C}(\text{CH}_3)_3$), 11.7 (s, $\text{C}_5(\text{CH}_3)_5$). MS (electrospray, CH_2Cl_2 solution): m/z 669–678 (M^+).

Synthesis of $[\text{Cp}^*\text{Mo}(\text{CO})_3\{\text{P}(\text{OC}_{10}\text{H}_{19})\text{C}(\text{Ph})\text{C}(\text{Ph})\}][\text{AlCl}_4] (\mathbf{8})$

$[\text{Cp}^*\text{Mo}(\text{CO})_3\{\text{P}(\text{Cl})(\text{OC}_{10}\text{H}_{19})\}] (\mathbf{6})$, 50 mg, 0.0931 mmol and diphenylacetylene (16.6 mg, 0.0931 mmol) were dissolved in CH_2Cl_2 (5 mL). The resulting solution was added to AlCl_3 (12 mg, 0.0931 mmol) and stirred for 30 min. The solvent volume was reduced under reduced pressure and pentane (10 mL) was added to the concentrated reaction solution with rapid stirring. The supernatant was removed and the resulting dark coloured oil was washed with pentane (5.0 mL) and dried under vacuum. Yield: 62.6 mg, 62.5%. IR (THF solution, $\nu(\text{CO})$, cm^{-1}): 2007 s, 1959 s, 1920 s. $^{31}\text{P}\{^1\text{H}\}$ NMR: δ -32.6. ^1H NMR: δ 7.48–6.89 (multiplets, Ph), 3.18 (multiplet, 1H, H_A menthol), 1.80–1.77 (multiplets, menthol), 1.76 (s, 15H, $\text{C}_5(\text{CH}_3)_5$), 1.75–0.53 (broad multiplets, menthol), 0.50 (d, 3H, $^3J_{\text{HH}} = 6.0$ Hz, $-\text{CH}(\text{CH}_3)_2$ (menthol)), 0.39 (d, 3H, $^3J_{\text{HH}} = 6.0$ Hz, CH_3 (menthol)), 0.01 (d, 3H, $^3J_{\text{HH}} = 9$ Hz, $\text{CH}(\text{CH}_3)_2$). ^{13}C NMR: δ 229.2 (s, MoCO), 226.5 (d, $J_{\text{CP}} = 8$ Hz, MoCO), 225.9 (s, MoCO), 148.0 (d, $J_{\text{PC}} = 18$ Hz, phosphirene ring C), 147.6 (d, $J_{\text{CP}} = 15$ Hz, phosphirene ring C), 133.0 (s, Ph), 132.8 (s, Ph), 130.4 (s, Ph), 130.2 (s, Ph), 129.7 (d, $J_{\text{CP}} = 6$ Hz, *o*-Ph), 129.3 (d, $J_{\text{CP}} = 6$ Hz, *o*-Ph), 129.1 (s, Ph), 128.7 (s, Ph), 127.2 (d, $J_{\text{CP}} = 3$ Hz, *ipso*-Ph), 126.8 (d, $J_{\text{CP}} = 3$ Hz, *ipso*-Ph), 109.7 (s, $\text{C}_5(\text{CH}_3)_5$), 79.9 (d, $J_{\text{CP}} = 15$ Hz, menthol C^1), 48.6 (d, $J_{\text{CP}} = 5$ Hz, menthol C^2), 42.6 (s, menthol C^6), 33.6 (s, menthol C^4), 31.8 (s, menthol C^5), 25.7 (s, menthol $\text{CH}(\text{CH}_3)_2$), 22.9 (s, menthol C^3), 22.0 (s, menthol CH_3), 21.2 (s, menthol $\text{CH}(\text{CH}_3)_2$), 16.0 (s, menthol $\text{C}(\text{CH}_3)_2$), 11.5 (s, $\text{C}_5(\text{CH}_3)_5$). MS (electrospray, THF solution): $m/z = 675$ – 684 (M^+).

X-ray crystallography

A suitable crystal of compound **3** was mounted on a glass fiber. Programs for diffractometer operation, data collection, cell indexing, data reduction and absorption correction were those supplied by Bruker AXS Inc., Madison, WI. Diffraction measurements were made on a PLATFORM diffractometer/SMART 1000 CCD using graphite-monochromated Mo- $K\alpha$ radiation at -80°C . The unit cell was determined from randomly selected reflections obtained using the SMART CCD automatic search, center, index and least-squares routines. Integration was carried out using the program SAINT and an absorption correction was performed using SADABS. Structure solution was carried out using the SHELX97 [36] suite of programs and the WinGX graphical interface [37]. Initial solutions were obtained by direct methods and refined by successive least-squares cycles. All non-hydrogen atoms were refined anisotropically.

Computational methods

Gas phase structures were optimized without any symmetry constraints using density functional theory (DFT), with a wave function incorporating the B3LYP exchange–correlation functional [27], as implemented in Gaussian 09 (revision C. 01) software package [34]. Basis set LANL2DZ was used for Mo and 6-31G(d,p) was used for all other atoms (C, H, O, N, P, Cl, and Al). Vibrational frequency analysis was used to confirm minima. Gaussian 09 was also used to compute NBO charges and isosurface plots [29]. The keywords used for optimization, vibrational, and NBO analyses are # *opt freq=noraman rb3lyp pop=(npa,full) gen pseudo=read*.

Additionally, single-point computations were performed to print the one electron integrals of all phosphinidene complexes and their fragments. The keywords used for this computation are #*P rb3lyp gen 5D NoSymm Pop=Full IOP(3/33=1) SCF=Tight (pseudo=read* is included only when a transition metal is present). The single-point output files, generated by Gaussian 09 software package, were used in the AOMix software package (revision 6.81) [31] to calculate Mayer bond orders [28] between atoms and to analyse the molecular orbital compositions in terms of contributions from fragment orbitals that was performed using Mulliken population analysis [35].

Acknowledgements

This work was financially supported by the University of Regina. We also thank Bob McDonald and Mike Ferguson (University of Alberta) for X-ray data collection.

Appendix A. Supplementary material

CCDC 982682 contains the supplementary crystallographic data for this paper. These data can be obtained free of charge from The Cambridge Crystallographic Data Centre via www.ccdc.cam.ac.uk/data_request/cif.

Appendix B. Supplementary data

Supplementary data related to this article can be found at <http://dx.doi.org/10.1016/j.jorganchem.2014.02.025>.

References

- [1] B.T. Sterenberg, K.A. Udachin, A.J. Carty, *Organometallics* 20 (2001) 2657–2659.
- [2] J. Sánchez-Nieves, B.T. Sterenberg, K.A. Udachin, A.J. Carty, *J. Am. Chem. Soc.* 125 (2003) 2404–2405.
- [3] (a) B.T. Sterenberg, K.A. Udachin, A.J. Carty, *Organometallics* 22 (2003) 3927–3932; (b) T.W. Graham, R.P.Y. Cariou, J. Sanchez-Nieves, A.E. Allen, K.A. Udachin, R. Regragui, A.J. Carty, *Organometallics* 24 (2005) 2023–2036.
- [4] R.A. Rajagopalan, B.T. Sterenberg, *Organometallics* 30 (2011) 2933–2938.
- [5] (a) A. Marinetti, F. Mathey, J. Fischer, A. Mitschler, *J. Am. Chem. Soc.* 104 (1982) 4484–4485; (b) F. Mathey, *Dalt. Trans.* (2007) 1861–1868; (c) M.L.G. Borst, R.E. Bulo, C.W. Winkel, D.J. Gibney, A.W. Ehlers, M. Schakel, M. Lutz, A.L. Spek, K. Lammertsma, *J. Am. Chem. Soc.* 127 (2005) 5800–5801.
- [6] (a) F. Mercier, B. Deschamps, F. Mathey, *J. Am. Chem. Soc.* 111 (1989) 9098–9100; (b) J.B.M. Wit, G.T. van Eijkel, F.J.J. de Kanter, M. Schakel, A.W. Ehlers, M. Lutz, A.L. Spek, K. Lammertsma, *Angew. Chem. Int. Ed.* 38 (1999) 2596–2599; (c) J.B.M. Wit, G.T. van Eijkel, M. Schakel, K. Lammertsma, *Tetrahedron* 56 (2000) 137–141; (d) M.L.G. Borst, R.E. Bulo, D.J. Gibney, Y. Alem, F.J.J. de Kanter, A.W. Ehlers, M. Schakel, M. Lutz, A.L. Spek, K. Lammertsma, *J. Am. Chem. Soc.* 127 (2005) 16985–16999; (e) M.L.G. Borst, N. van der Riet, R.H. Lemmens, F.J.J. de Kanter, M. Schakel, A.W. Ehlers, A.M. Mills, M. Lutz, A.L. Spek, K. Lammertsma, *Chem. Eur. J.* 11 (2005) 3631–3642.
- [7] S. Holand, F. Mathey, *Organometallics* 7 (1988) 1796–1801.
- [8] M.P. Duffy, F. Mathey, *J. Am. Chem. Soc.* 131 (2009) 7534–7535.
- [9] C. Compain, B. Donnadiou, F. Mathey, *Organometallics* 25 (2006) 540–543.
- [10] (a) R. Grubba, K. Baranowska, J. Chojnacki, J. Pikies, *Eur. J. Inorg. Chem.* 2012 (2012) 3263–3265; (b) W. Domanska-Babul, J. Chojnacki, E. Matern, J. Pikies, *Dalt. Trans.* (2009) 146–151; (c) J. Pikies, E. Baum, E. Matern, J. Chojnacki, R. Grubba, A. Robaszekiewicz, *Chem. Commun.* (2004) 2478–2479; (d) J. Olkowska-Oetzel, J. Pikies, *Appl. Organomet. Chem.* 17 (2003) 28–35.
- [11] (a) B.T. Sterenberg, O.S. Senturk, K.A. Udachin, A.J. Carty, *Organometallics* 26 (2007) 925–937; (b) K. Vaheesar, T.M. Bolton, A.L.L. East, B.T. Sterenberg, *Organometallics* 29 (2010) 484–490.
- [12] (a) T.W. Graham, K.A. Udachin, A.J. Carty, *Chem. Commun.* (2005) 5890–5892; (b) T.W. Graham, K.A. Udachin, M.Z. Zgierski, A.J. Carty, *Can. J. Chem.* 85 (2007) 885–888.

- [13] R. Maisch, M. Barth, W. Malisch, J. Organomet. Chem. 260 (1984) C35–C39.
- [14] (a) E.A.V. Ebsworth, R.O. Gould, N.T. McManus, N.J. Pilkington, D.W.H. Rankin, J. Chem. Soc. Dalt. Trans. (1984) 2561–2567;
(b) L. Weber, H. Misiak, H.G. Stammler, B. Neumann, Z. Anorg. Allg. Chem. 620 (1994) 1730–1735.
- [15] L. Weber, L. Pumpenmeier, H.-G. Stammler, B. Neumann, Dalt. Trans. (2004) 659–667.
- [16] (a) L. Weber, U. Sonnenberg, H.G. Stammler, B. Neumann, Z. Naturforsch. B 46 (1991) 714–718;
(b) L. Weber, U. Sonnenberg, Chem. Ber. 124 (1991) 725–728;
(c) W. Malisch, K. Jörg, E. Gross, M. Schmeusser, A. Meyer, Phosphorus Sulfur Relat. Elem. 26 (1986) 25–29;
(d) E.A.V. Ebsworth, N.T. McManus, N.J. Pilkington, D.W.H. Rankin, J. Chem. Soc. Chem. Commun. (1983) 484–485.
- [17] K.B. Dillon, F. Mathey, J.F. Nixon, Phosphorus: The Carbon Copy, John Wiley & Sons, Ltd., Chichester, 1998, p. 30.
- [18] A. Schmidpeter, S. Lochschmidt, W.S. Sheldrick, Angew. Chem. Int. Ed. Engl. 24 (1985) 226–227.
- [19] P. Leoni, E. Aquilini, M. Pasquali, F. Marchetti, M. Sabat, J. Chem. Soc. Dalt. Trans. (1988) 329–333.
- [20] K. Vaheesar, C.M. Kuntz, B.T. Sterenberg, J. Organomet. Chem. 745–746 (2013) 347–355.
- [21] (a) A.W. Ehlers, E.J. Baerends, K. Lammertsma, J. Am. Chem. Soc. 124 (2002) 2831–2838;
(b) G. Frison, F. Mathey, A. Sevin, J. Organomet. Chem. 570 (1998) 225–234.
- [22] (a) A.W. Ehlers, K. Lammertsma, E.J. Baerends, Organometallics 17 (1998) 2738–2742;
(b) S. Grigoleit, A. Alijah, A.B. Rozhenko, R. Streubel, W.W. Schoeller, J. Organomet. Chem. 643–644 (2002) 223–230;
(c) J.-G. Lee, J.E. Boggs, A.H. Cowley, Polyhedron 5 (1986) 1027–1029;
(d) S. Creve, K. Pierloot, M.T. Nguyen, Chem. Phys. Lett. 285 (1998) 429–437.
- [23] S. Creve, K. Pierloot, M.T. Nguyen, L.G. Vanquickenborne, Eur. J. Inorg. Chem. (1999) 107–115.
- [24] (a) H. Aktaş, J.C. Slootweg, A.W. Ehlers, M. Lutz, A.L. Spek, K. Lammertsma, Organometallics 28 (2009) 5166–5172;
(b) A.T. Termaten, T. Nijbacker, A.W. Ehlers, M. Schakel, M. Lutz, A.L. Spek, M.L. McKee, K. Lammertsma, Chem. Eur. J. 10 (2004) 4063–4072;
(c) A.T. Termaten, H. Aktas, M. Schakel, A.W. Ehlers, M. Lutz, A.L. Spek, K. Lammertsma, Organometallics 22 (2003) 1827–1834;
(d) G. Zhao, F. Basuli, U.J. Kilgore, H. Fan, H. Aneetha, J.C. Huffman, G. Wu, D.J. Mindiola, J. Am. Chem. Soc. 128 (2006) 13575–13585;
(e) F. Basuli, B.C. Bailey, J.C. Huffman, M.H. Baik, D.J. Mindiola, J. Am. Chem. Soc. 126 (2004) 1924–1925.
- [25] K.K. Pandey, P. Tiwari, P. Patidar, J. Organomet. Chem. 740 (2013) 135–140.
- [26] (a) K.K. Pandey, A. Liedós, J. Organomet. Chem. 695 (2010) 206–214;
(b) K.K. Pandey, P. Tiwari, P. Patidar, J. Phys. Chem. A 116 (2012) 11753–11762;
(c) K.K. Pandey, P. Tiwari, P. Patidar, S.K. Patidar, R. Vishwakarma, P.K. Bariya, J. Organomet. Chem. 751 (2014) (2013) 781–787.
- [27] (a) A.D. Becke, Phys. Rev. A 38 (1988) 3098–3100;
(b) J.P. Perdew, Phys. Rev. B 33 (1986) 8822–8824.
- [28] I. Mayer, Chem. Phys. Lett. 97 (1983) 270–274.
- [29] A.E. Reed, R.B. Weinstock, F. Weinhold, J. Chem. Phys. 83 (1985) 735–746.
- [30] J. Rusanova, E. Rusanov, S.I. Gorelsky, D. Christendat, R. Popescu, A.A. Farah, R. Beaulac, C. Reber, A.B.P. Lever, Inorg. Chem. 45 (2006) 6246–6262.
- [31] S.I. Gorelsky, AOMix Software, University of Ottawa, Ottawa, ON, 2013.
- [32] M.T. Nguyen, A. Van Keer, L.G. Vanquickenborne, J. Org. Chem. 61 (1996) 7077–7084.
- [33] (a) C. Hering, A. Schulz, A. Villinger, Inorg. Chem. 52 5214–5225; (b) A.H. Cowley, R.A. Kemp, Chem. Rev. 85 (1985) 367–382.
- [34] M.J. Frisch, G.W. Trucks, H.B. Schlegel, G.E. Scuseria, M.A. Robb, J.R. Cheeseman, G. Scalmani, V. Barone, B. Mennucci, G.A. Petersson, H. Nakatsuji, M. Caricato, X. Li, H.P. Hratchian, A.F. Izmaylov, J. Bloino, G. Zheng, J.L. Sonnenberg, M. Hada, M. Ehara, K. Toyota, R. Fukuda, J. Hasegawa, M. Ishida, T. Nakajima, Y. Honda, O. Kitao, H. Nakai, T. Vreven, J. Montgomery, J. A., J.E. Peralta, F. Ogliaro, M. Bearpark, J.J. Heyd, E. Brothers, K.N. Kudin, V.N. Staroverov, R. Kobayashi, J. Normand, K. Raghavachari, A. Rendell, J.C. Burant, S.S. Iyengar, J. Tomasi, M. Cossi, N. Rega, J.M. Millam, M. Klene, J.E. Knox, J.B. Cross, V. Bakken, C. Adamo, J. Jaramillo, R. Gomperts, R.E. Stratmann, O. Yazyev, A.J. Austin, R. Cammi, C. Pomelli, J.W. Ochterski, R.L. Martin, K. Morokuma, V.G. Zakrzewski, G.A. Voth, P. Salvador, J.J. Dannenberg, S. Dapprich, A.D. Daniels, Ö. Farkas, J.B. Foresman, J.V. Ortiz, J. Cioslowski, D.J. Fox, Gaussian 09, Revision C. 01, Gaussian, Inc., Wallingford CT, 2009.
- [35] (a) R.S. Mulliken, J. Chem. Phys. 23 (1955) 1833–1840;
(b) R.S. Mulliken, J. Chem. Phys. 23 (1955) 1841–1846.
- [36] G.M. Sheldrick, Release, 97-2 ed., 1998.
- [37] L.J. Farrugia, Appl. Cryst. 32 (1999) 837–838.